Maglad *et al. Int J Concr Struct Mater* (2023) 17:74
https://doi.org/10.1186/s40069-023-00637-w

International Journal of Concrete Structures and Materials

RESEARCH

Open Access

Experimental and Analytical Investigation of Fracture Characteristics of Steel Fiber-Reinforced Recycled Aggregate Concrete

Ahmed M. Maglad[1], Walid Mansour[2*], Bassam A. Tayeh[3], Mohamed Elmasry[4], Ahmed M. Yosri[5] and Sabry Fayed[2]

Abstract

Fracture parameters of fiber concrete (FC) are currently a hot research area. Fracture mechanics is the field of solid mechanics that helps to study the type and propagation of cracks in materials. It uses methods of calculating the driving force on a crack and characterizes the material's resistance to fracture. Behavioral characteristics are determined by crack mouth opening displacement and the load–deflection method. This research identifies the fracture parameters of 33 notched simply supported beams made by recycled aggregate cement concrete with steel fiber. The recycled aggregate ratio in concrete has been altered to determine the effect on the mechanical and fracture properties. For determining fracture parameters, a 3-point bending single-edge notched fracture test was used. The results indicated that the steel fiber-reinforced concrete made with recycled aggregate showed similar performance and fracture characteristics compared to normal concrete. Thus, adding steel fibers to various concrete mixes considerably improved the fracture characteristics, while the brittleness was reduced with increased steel fiber content. Linear regression analysis also showed the accuracy of mechanical strength results as the value of R-square was close to unity. Displacement, ultimate load, brittleness (B), fracture toughness (K_{IC}), crack mouth opening displacement (CMOD), fracture energy (G_F), modulus of elasticity (E), and characteristic length (l_{ch}), were determined for both conventional and recycled aggregate specimens. The "work of fracture"—by definition the formula—is the most reliable to calculate the fracture energy as the nonlinearity is related to the performance of FC.

Keywords Recycled aggregate, Fracture mechanics, Steel fiber, Fracture toughness, Fracture energy, Notched beam

Journal information: ISSN 1976-0485 / eISSN 2234-1315.

*Correspondence:
Walid Mansour
waled_mansour@eng.kfs.edu.eg
[1] Department of Civil Engineering, Najran University, Najran, Saudi Arabia
[2] Civil Engineering Department, Faculty of Engineering, Kafrelsheikh University, Kafrelsheikh, Egypt
[3] Civil Engineering Department, Faculty of Engineering, Islamic University of Gaza, Gaza, Palestine
[4] High Institute of Engineering, Elshorouk Academy, Cairo, Egypt
[5] Civil Engineering Department, Faculty of Engineering, Delta University for Science and Technology, Belkas, Egypt

1 Introduction

Failure of structural members often causes cracking that ultimately causes catastrophic events, although the stress level is pre-considered and signifies a good design. Studying the instigation and spreading of structural cracking is a multifaceted objective that indicates various concepts from engineering mechanics, chemistry, and physics. Fracture mechanics explores the response and failure of structures due to the initiation and spreading of cracks. ACI Committee 446.1 R-91 (ACI Committee, 1991) explained the FM as a type of failure theory that utilizes energy criteria, probably in combination with strength criteria, to justify the spreading of cracks over a building. It uses the linear elastic method to evaluate the driving force of the cracking and empirical engineering mechanics theories to describe the resistance of a material against fracture. In concrete, which is brittle, a huge fracture process zone is generally developed in the face of cracking-like failure, which absorbs a high quantity of energy before the concrete's failure.

2 Literature Review

Sustainable construction means designing a structure with suitable durability throughout its stated service life. If the vision of a sustainable material flow is to be realized, the quantity of recycled waste has to be augmented. Specifically, the building sector is a leading user of materials and, simultaneously, the leading maker of waste materials (ACI Committee, 1991). Obtaining coarse aggregates from the buildings' waste and demolition material (WDM) is the commonly adopted way to attain eco-friendly concrete. This lowers the use of raw materials and reduces the stress on landfills. Hence, utilizing recycled coarse aggregates (RCA) in making fresh concrete seems to be an effective method of using WDM. The mechanical strength of concrete made with RCA must be further studied before its real-life usage in buildings (Rajhans et al., 2019). Presently, there are fewer studies on the fracture performance of concrete made with RCA. Accessible empirical results regarding recycled aggregate concrete (RAC) are highly inconsistent, as the quality of RAC generally relies on the quality of the parental concrete obtained from the WDM (Corinaldesi & Moriconi, 2009; Pedro et al., 2017). In addition to the variation in the arrangement of RCA, the shortage of data and results regarding the structure's response of its members with recycled aggregate concrete is one more feature that limits its usage in the building sector. Though the utilization of WDM as an RCA in the replacement of natural stone aggregates has shown an appropriate answer to reduce the use of raw materials (Kurad et al., 2017; Singh & Singh, 2016; Xie et al., 2015), the microstructural response of the RAC is not entirely understood by the researchers yet. The building codes and various national standards restrict its utilization in the building sector. The author of a study researched the rough surface of RCA and revealed that it allows excellent mechanical linking amid the binder's matrix and grains because of the infiltration of the binder's paste with steel fiber (SFs) into the surface pores in the grains of RCA (Chaboki et al., 2018). The utilization of RCA in concrete raises shrinkage as the recycled coarse aggregates ingest an immense amount of water. Adding (SFs) to develop fiber-reinforced recycled aggregate concrete effectively decreases drying shrinkage, autogenous shrinkage, and related cracks. The high elastic modulus of steel fiber can reduce crack width and delay crack propagation during the shrinkage development process. It also improves the concrete's energy absorption capability (Aflaki Samani & Jabbari Lak, 2019; Baena et al., 2016; Basha et al., 2020; Carneiro et al., 2014; Liu et al., 2018; Mansour & Fayed, 2021a). Moreover, it is a well-known fact that the addition of SFs could improve the strength and fracture characteristics, resistance against spalling, and toughness of conventional concrete. A research study was performed to observe the fracture response counting fracture toughness, energy, and rate of energy release of RCA with various substitution levels of recycled aggregates. Using RCA in conventional concrete could be labeled as protecting the environment and atmosphere (Mansour et al., 2022a).

2.1 Research Novelty

In this study, the range of the recycled coarse aggregate ratio up to 100% as a partial substitute for natural stone coarse aggregate was investigated. According to the authors, no significant research study has been conducted on this topic, which shows the novelty of the current study. This research deals with the strength and fracture characteristics, modulus of rupture, fracture toughness, and fracture energy of concrete. The present study will increase awareness among researchers and readers about the fracture toughness, fracture energy, modulus of elasticity, and strength characteristics of steel fibers reinforced recycled aggregate concrete. To perform the research, eleven types of concrete mixes were prepared and tested in the lab, where concrete with natural stone coarse aggregates was kept as a reference. Ten mixtures of concrete were prepared with RCA from a 10 to 100% substitution ratio.

3 Experimental Plan

The experimental plan was developed to examine the fracture response of notched beam samples with various recycle aggregate replacement ratios in concrete mixes made of different steel fiber ratios, which were classified into three sets. The first set deals with notched beams made with a 0.5% steel fiber ratio (NC-SF0.5, RC10-SF0.5 to RC100-SF0.5). The second set deals with notched beams of 1% steel fiber ratio (NC-SF1.0, RC10-SF1.0 to RC100-SF1.0). The third group deals with a 1.5% steel fiber ratio (NC-SF1.5, RC10-SF1.5 to RC100-SF1.5).

3.1 Materials

For the present study, Type I, grade 42.5 Portland cement, according to ASTM C 150 (Mansour, 2021), was utilized in mixtures as essential binders and had a specific surface area of 2500 cm^2/g and a specific gravity of 2.34. For aggregates, medium-sized, well-graded fine aggregate with a fineness modulus of 2.5 and passing through a sieve size of 4.75 mm was used. Natural stone coarse aggregates of 10 mm maximum size with a specific gravity of 2.51 were utilized. Coarse and fine aggregates followed the ASTM C 33 standards (Althoey et al., 2022).

Recycled aggregate (RCA)—old crushed concrete of 10 mm nominal size with a specific gravity of 2.49 and a water absorption of 4.70% was utilized as recycled coarse aggregate. Particle size distribution curves for fine, coarse, and recycled coarse aggregates are provided in Fig. 1. For fibers, end-hooked steel fibers (SF) as shown in Fig. 2 with 0.8 mm and 35 mm equivalent diameters and lengths were used with 0.5%, 1.0%, and 1.5% as volume fractions. For water (W)- Tap water followed the criteria of ECP 203–2019 (ASTM Annual Book of Standards, 2004) and was used in all concrete mixes. For admixture, Type G high range water reducing admixture was used following ASTM C 494 (ASTM-C33 2023) at 5% by cement's mass.

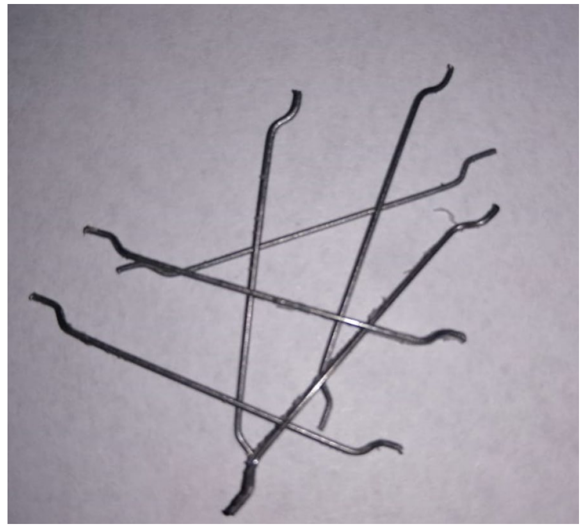

Fig. 2 Hooked end steel fibers

3.2 Test Procedures and Specimens Preparation

Thirty-three mixes of samples were prepared to investigate the current research plan. Entire mixtures were made with fine aggregate: total coarse aggregate ratio of 1:1.8:3.6 and water/cement of 0.42 to achieve appropriate workability. Table 1 provides the mixes proportions. The mixtures are termed by codes: (N) for concrete with normal aggregate and (R) for concrete with recycled aggregate—% recycled aggregate ratio—% steel fibers, respectively. For concrete mixes, first water and admixture were mixed. Then mix the cement, sand, and CA + RC with various percentages in a dry condition for 1 min. Then, the liquid was introduced to the previously mixed solid particles to obtain a uniform and workable slurry. Lastly, steel fibers were slowly introduced to the mixture, and mixing was sustained for at least 3 min until the mixture was glossy and well combined. After casting, the samples were covered and kept at an ambient temperature of 22 ± 3 °C and 55% relative humidity for one day. After that, samples were placed in water for curing at 22 ± 3 °C till the testing day. Samples were prepared in cubes of 100 mm, × 100 mm × 100 mm for compression strength, a 100 mm × 200 mm concrete mold for modulus of elasticity and split tensile strength, and 100 mm × 100 mm × 500 mm beams for flexural strength. The mechanical characteristics of the concrete samples were tested during the curing phase of 28 days. The target compressive strength of conventional concrete was 20 MPa. A hydraulic testing machine with a total capability of 2000 kN was utilized for testing cylinder and cube samples according to BS EN 12390-2019 (HBRC & Cairo, 2019, EN BS 2002) and ASTM C 469 (ASTM, 2013, ASTM C 2011), respectively. Thirty-three beam specimens of 100 × 100 × 500 mm with a notch were used, and the notches were made at the lower surface of the middle of 3 mm width and 20 mm height. Geometry, setup details, and specimen preparation are detailed in Figs. 3 and 4, respectively. Every beam sample was tried after 28 days, utilizing a 300-kN servo-controlled UTM under displacement control and a loading rate of 0.05 mm/min. The

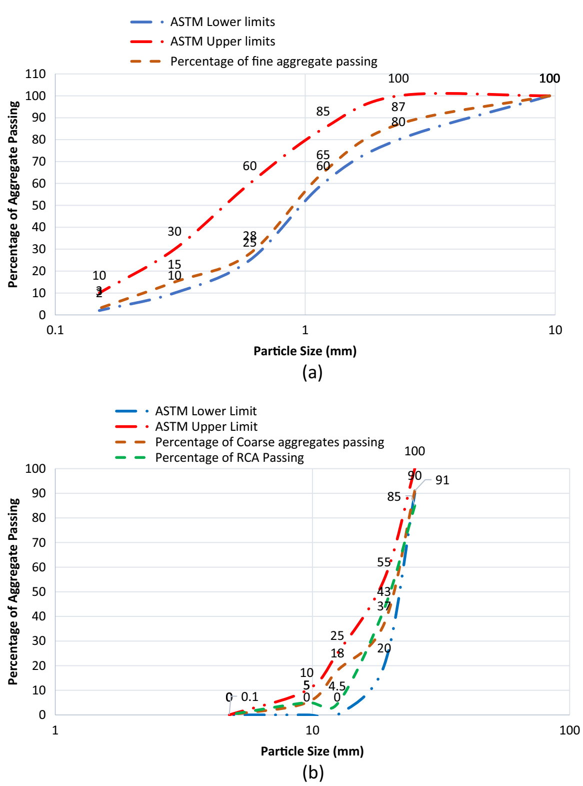

Fig. 1 Particle size distribution curve: **a** fine aggregate, **b** coarse and recycled coarse aggregate

Table 1 Concrete mix proportions (kg/m^3)

Group	Specimen ID	Recycled aggregate (RA)	Natural aggregate (CA)	OPC	Sand	Water	Admixture	(SFs)
G1	NC-SF0.5	0	1300	360	650	150	20	39.25
	RC10-SF0.5	130	1170	360	650	150	20	39.25
	RC20-SF0.5	260	1040	360	650	150	20	39.25
	RC30-SF0.5	390	910	360	650	150	20	39.25
	RC40-SF0.5	520	780	360	650	150	20	39.25
	RC50-SF0.5	650	650	360	650	150	20	39.25
	RC60-SF0.5	780	520	360	650	150	20	39.25
	RC70-SF0.5	910	390	360	650	150	20	39.25
	RC80-SF0.5	1040	260	360	650	150	20	39.25
	RC90-SF0.5	1170	130	360	650	150	20	39.25
	RC100-SF0.5	1300	0	360	650	150	20	39.25
G2	NC-SF1.0	0	1300	360	650	150	20	78.5
	RC10-SF1.0	130	1170	360	650	150	20	78.5
	RC20-SF1.0	260	1040	360	650	150	20	78.5
	RC30-SF1.0	390	910	360	650	150	20	78.5
	RC40-SF1.0	520	780	360	650	150	20	78.5
	RC50-SF1.0	650	650	360	650	150	20	78.5
	RC60-SF1.0	780	520	360	650	150	20	78.5
	RC70-SF1.0	910	390	360	650	150	20	78.5
	RC80-SF1.0	1040	260	360	650	150	20	78.5
	RC90-SF1.0	1170	130	360	650	150	20	78.5
	RC100-SF1.0	1300	0	360	650	150	20	78.5
G3	NC-SF1.5	0	1300	360	650	150	20	117.75
	RC10-SF1.5	130	1170	360	650	150	20	117.75
	RC20-SF1.5	260	1040	360	650	150	20	117.75
	RC30-SF1.5	390	910	360	650	150	20	117.75
	RC40-SF1.5	520	780	360	650	150	20	117.75
	RC50-SF1.5	650	650	360	650	150	20	117.75
	RC60-SF1.5	780	520	360	650	150	20	117.75
	RC70-SF1.5	910	390	360	650	150	20	117.75
	RC80-SF1.5	1040	260	360	650	150	20	117.75
	RC90-SF1.5	1170	130	360	650	150	20	117.75
	RC100-SF1.5	1300	0	360	650	150	20	117.75

NC natural aggregate concrete, *RC* recycled aggregate concrete

RC10, RC20, RC30, RC40, RC50, RC60, RC70, RC80, RC90, and RC100; denote the recycled aggregate substitution ratios by weight at 10%, 20%, 30%, 40%, 50%, 60%, 70%, 80%, 90%, and 100%, respectively; and SF0.5, SF1.0, and SF1.5 denote the steel fiber volume fraction ratios at 0.5%, 1.0%, and 1.5%, respectively

30-mm LVDT recorded the vertical displacement and used a 50 ± 4 mm Pi-gauge to record crack mouse opening displacement (CMOD). The experimental tests were carried out in the reinforced concrete laboratory of the faculty of engineering at Kafrelsheikh University, Egypt.

4 Test Results and Discussion

4.1 Mechanical Properties

The results for the strength characteristics of different concrete mixtures after 28 days are presented in Table 2. A decrease in the concrete's compression strength is noticed in Fig. 5 by raising the recycled concrete aggregates' substitution level. For example, standard/control concrete's compression strength was 20.8 MPa, but it was reduced to 14.3 MPa with the substitution of 100% RCA. A reduction in the compression strength of recycled aggregate concrete could be ascribed to the mortar attached to the recycled aggregates. A decrease in the mechanical strength of recycled aggregate concrete could be associated with various terms, such as the level of recycled aggregate substitution and the mixture's water-to-binder ratio (Kapoor et al., 2016; Hamoda et al., 2019; Sakr et al., 2018; Baraghith et al., 2022; Fayed

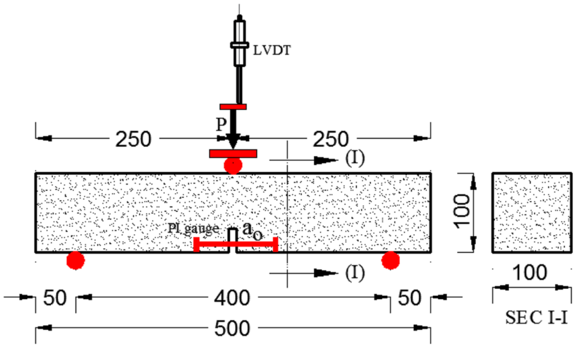

Fig. 3 Geometry and setup of the three-point bending test (dimensions are in mm)

(a)

(b)

Fig. 4 **a** Beams preparation and **b** test samples in cylinders

and Mansour 2020; Mansour and Fayed 2021b; Mansour et al., 2022b;Fayed et al., 2022; Ali et al., 2021; Masood et al., 2020; Pepe et al., 2014; Zaid et al., 2022a; Afroughsabet et al., 2017). No considerable impact on concrete's strength was noted for up to 30% substitution of recycled aggregates. The decrease in compressive strength of concrete ranged from 3 to 10% compared to reference samples that do not contain recycled aggregates. On the contrary, a more significant decrease (12–33%) in mechanical strength was indicated by raising the substitution level of recycled aggregates higher than 30%. The moisture conditions of recycled aggregates also impact the compression strength of recycled aggregate concrete. Due to the attached mortar in the recycled aggregates, the recycled aggregate concrete requires more water than standard concrete because the attached mortar absorbs some of the water. Hence, extra water is necessary to compensate for the absorbed water.

Similarly, for the result of splitting tensile strength, the trend of reduction in strength is also noticed in Fig. 6, as the standard/control concrete's splitting tensile strength was 2.71 MPa, but it was reduced to 2.20 MPa with the substitution of 100% RCA. This reduction in strength could be attributed to the porous mortar attached to the recycled aggregate's surface. Surface properties, strength, and quality of the parental concrete from which the recycled aggregates are derived are also essential factors that govern the strength of recycled aggregate concrete. Hence, the reduction in strength is also ascribed to the low quality and strength of recycled aggregates, which led to a decrease in splitting tensile strength. But with the addition of steel fibers, the reduction in splitting tensile strength was much lower than the compression strength, as the steel fibers acted as a fiber bridging material and averted the propagation of cracks, which ultimately prevented the recycled aggregates from degrading the splitting tensile strength of steel fibers reinforced recycled aggregate concrete.

As the compressive strength is the most important strength property of concrete, it is necessary that strength properties such as splitting tensile strength, flexural strength, and modulus of elasticity all have homogenous and uniform values in relation to the compression strength. A linear regression statistical analysis was performed to evaluate the compression strength of concrete at 28 days by utilizing the values of splitting tensile and flexural strength. It can be noted from Fig. 7 that both the R-square values of split tensile and flexural strength were more than 90% (91.8% and 99.2%) and reached unity, which shows the accuracy of the present results of the mechanical characteristics of steel fiber-reinforced recycled aggregate concrete.

4.2 Flexural Behavior

The beam specimen's results are given in Table 3. As observed from the results of the flexural strength test, the concrete samples are failing at low Max load as the percentage of recycled aggregates increases. Also, the flexural strength for standard concrete was 10.97 MPa, which was reduced to 2.37 MPa for the 100% substitution of recycled

Table 2 Mechanical properties of mixes at 28 days of curing

Group	Specimen ID	Compressive strength (MPa)	Splitting tensile strength (MPa)	Flexural strength (MPa)	Modulus of elasticity (GPa)
G1	NC-SF0.5	20.8	2.71	10.97	48.76
	RC10-SF0.5	20.1	2.66	8.66	57.72
	RC20-SF0.5	19.4	2.62	7.80	53.33
	RC30-SF0.5	18.7	2.57	6.98	49.00
	RC40-SF0.5	18.2	2.53	5.79	48.21
	RC50-SF0.5	17.6	2.48	4.37	37.58
	RC60-SF0.5	16.8	2.43	3.93	40.31
	RC70-SF0.5	16.7	2.40	3.47	37.03
	RC80-SF0.5	15.9	2.37	2.81	25.87
	RC90-SF0.5	15.1	2.30	2.49	23.33
	RC100-SF0.5	14.3	2.21	2.37	21.10
G2	NC-SF1.0	21.4	2.75	13.96	37.24
	RC10-SF1.0	20.8	2.71	13.27	36.14
	RC20-SF1.0	19.9	2.65	11.97	40.76
	RC30-SF1.0	19.1	2.6	10.17	38.76
	RC40-SF1.0	18.8	2.58	9.18	37.65
	RC50-SF1.0	17.9	2.51	7.60	31.67
	RC60-SF1.0	17.3	2.47	6.58	29.75
	RC70-SF1.0	16.5	2.39	5.73	27.76
	RC80-SF1.0	15.9	2.36	4.81	24.66
	RC90-SF1.0	15.1	2.29	3.89	20.75
	RC100-SF1.0	14.5	2.20	3.47	18.51
G3	NC-SF1.5	23.5	2.88	15.66	26.26
	RC10-SF1.5	22.9	2.85	15.22	26.27
	RC20-SF1.5	22.4	2.80	14.62	30.00
	RC30-SF1.5	21.8	2.77	14.00	32.47
	RC40-SF1.5	21.1	2.71	12.91	30.46
	RC50-SF1.5	20.3	2.68	10.53	26.23
	RC60-SF1.5	18.9	2.58	9.64	24.47
	RC70-SF1.5	17.7	2.48	6.98	20.69
	RC80-SF1.5	17.1	2.45	4.59	14.39
	RC90-SF1.5	16.8	2.40	3.89	12.97
	RC100-SF1.5	15.9	2.35	3.95	15.05

coarse aggregates. The bonding strength amid the paste of cement and aggregates plays a vital role in improving the concrete's flexural strength. Different types of impurities in recycled aggregates, such as particles of old concrete, play their part in lowering the flexural strength of recycled aggregate concrete because of its poor adhesive properties with the paste of cement. The results of the current study showed a 3–36% reduction in flexural strength of recycled aggregate concrete with a replacement ratio lower than 40% with respect to natural aggregate concrete. As the content of the recycled aggregates increased from 40% up to 100%, the flexural strength of recycled aggregate concrete was 18–79% lower than conventional concrete, depending on the steel fiber ratio within the mixture. Due to the crack stitching effect of steel fibers, further degrading of the flexural strength of recycled aggregate concrete was prevented. The steel fibers hold the concrete matrix tighter, which ultimately improves the flexural behavior of concrete with recycled aggregates (Ahmadi & Farzin, 2017; Sagoe-Crentsil et al., 2001; Zaid et al., 2022b).

4.3 Load–Deflection Behavior

Fig. 8 shows the load–deflection relationship of beam specimens. It could be concluded from Fig. 3 that the beam sample with 0.5% steel fiber failed in a brittle pattern; once the sample arrived at the highest load, the

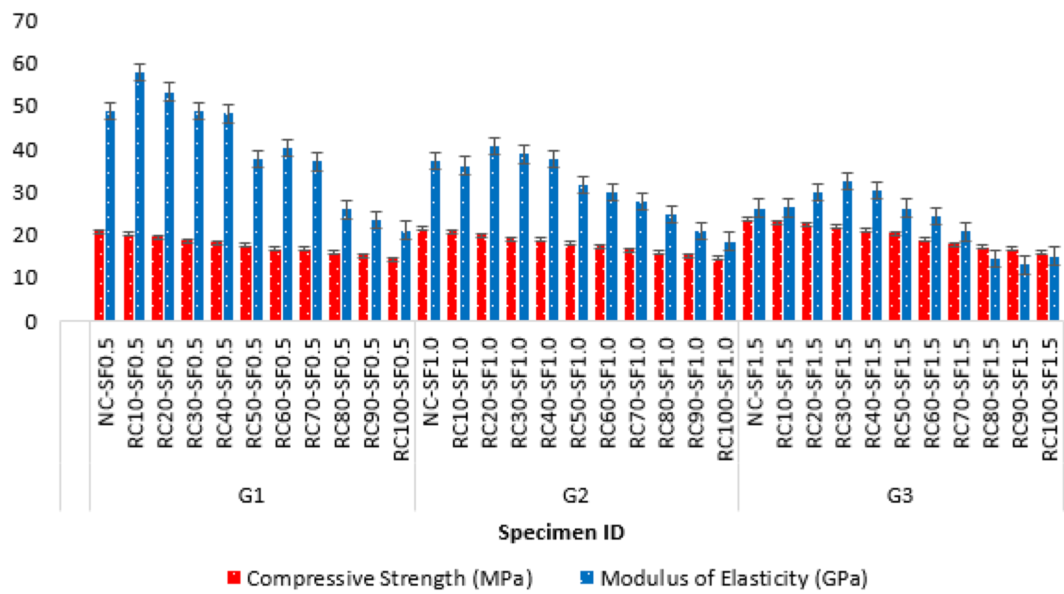

Fig. 5 Compressive strength and modulus of elasticity of samples at 28 days

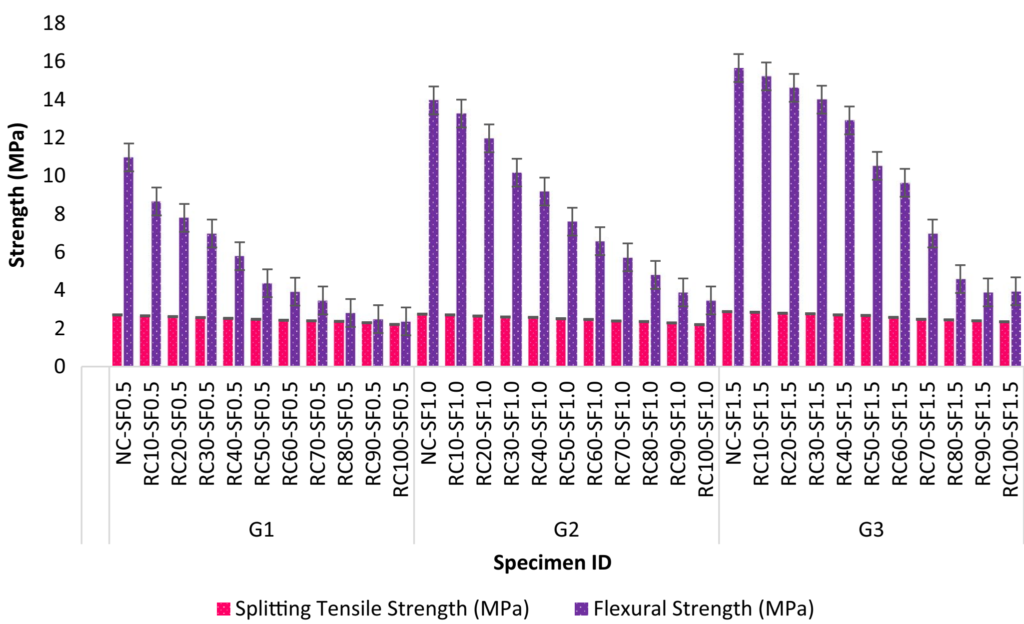

Fig. 6 Splitting tensile and flexural strength of samples at 28 days

load reduced quickly with low energy absorption. At the same time, the sample of the beam with 1.5% steel fibers failed in a ductile mode. From Fig. 8, it can be seen that the vital role of the steel fibers on the load–deflection response is to shift the brittle mode to a ductile manner in which the combination of steel fiber promotes tensile and flexural strength. As the applied loading on the notched concrete beam was raised, no cracking was noted until the maximum loading. From the flexure test on a single notched beam, it could be explained that the notch started to spread with increased loads. When the load reached its peak value, the notch started to propagate quickly in the ligament at its end. The cracking opened quicker in the samples, including a comparatively low steel fiber. A failure happened by opening an individual crack in the ligament, as presented in Fig. 9. The test

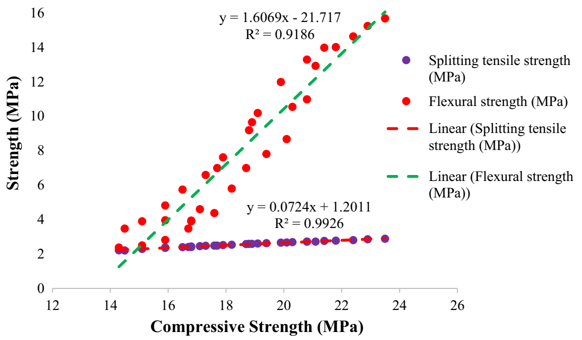

Fig. 7 Linear regression analysis of mechanical properties of samples

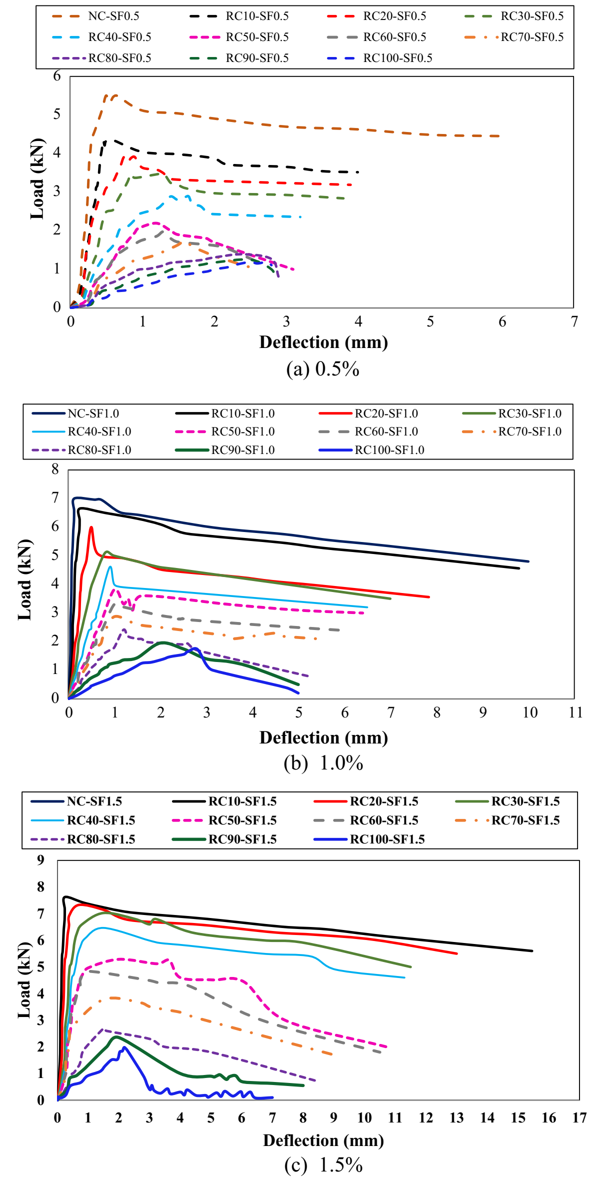

Fig. 8 Load- Deflection behavior of beam samples reinforced with different steel fibers ratios: (**a**) 0.5%, (**b**) 1.0%, and(**c**) 1.5%

Table 3 Flexural test outcome of beam samples

Group	Specimen ID	Max. load (kN.)	Max. deflection (mm)	CMOD (mm)
G1	NC-SF0.5	5.50	6.00	1.69
	RC10-SF0.5	4.34	4.00	2.41
	RC20-SF0.5	3.91	3.90	1.69
	RC30-SF0.5	3.50	3.80	1.69
	RC40-SF0.5	2.90	3.20	2.18
	RC50-SF0.5	2.19	3.10	1.93
	RC60-SF0.5	1.97	2.60	2.65
	RC70-SF0.5	1.74	2.50	2.89
	RC80-SF0.5	1.41	2.90	3.14
	RC90-SF0.5	1.25	2.85	3.62
	RC100-SF0.5	1.19	3.00	3.62
G2	NC-SF1.0	7.00	10.00	1.69
	RC10-SF1.0	6.65	9.79	1.69
	RC20-SF1.0	6.00	7.83	1.69
	RC30-SF1.0	5.10	7.00	1.93
	RC40-SF1.0	4.60	6.50	2.18
	RC50-SF1.0	3.81	6.40	2.18
	RC60-SF1.0	3.30	5.90	2.41
	RC70-SF1.0	2.87	5.50	2.89
	RC80-SF1.0	2.41	5.20	2.89
	RC90-SF1.0	1.95	5.00	3.38
	RC100-SF1.0	1.74	5.00	3.86
G3	NC-SF1.5	7.85	15.90	1.51
	RC10-SF1.5	7.63	15.45	1.69
	RC20-SF1.5	7.33	13.00	1.69
	RC30-SF1.5	7.02	11.50	1.69
	RC40-SF1.5	6.47	11.30	1.69
	RC50-SF1.5	5.28	10.71	1.69
	RC60-SF1.5	4.83	10.50	1.93
	RC70-SF1.5	3.50	9.00	1.93
	RC80-SF1.5	2.30	8.50	1.93
	RC90-SF1.5	1.95	8.00	2.17
	RC100-SF1.5	1.98	7.00	2.41

outcomes of the highest loads and maximum mid-span deflection for various samples of beams are depicted in Table 3 and illustrated in Fig. 10. The impact of utilizing different recycled aggregate replacements (0%, 10%, 20%, 30%, 40%, 50%, 60%, 70%, 80%, 90%, and 100%) was studied through beam specimens (NR, RC10 to RC100), correspondingly as depicted in Fig. 10. From Fig. 10a, it could be observed that enhancing the substitution level of recycled aggregate reduced the highest load by 76% for all specimens with various steel fiber ratios. Raising

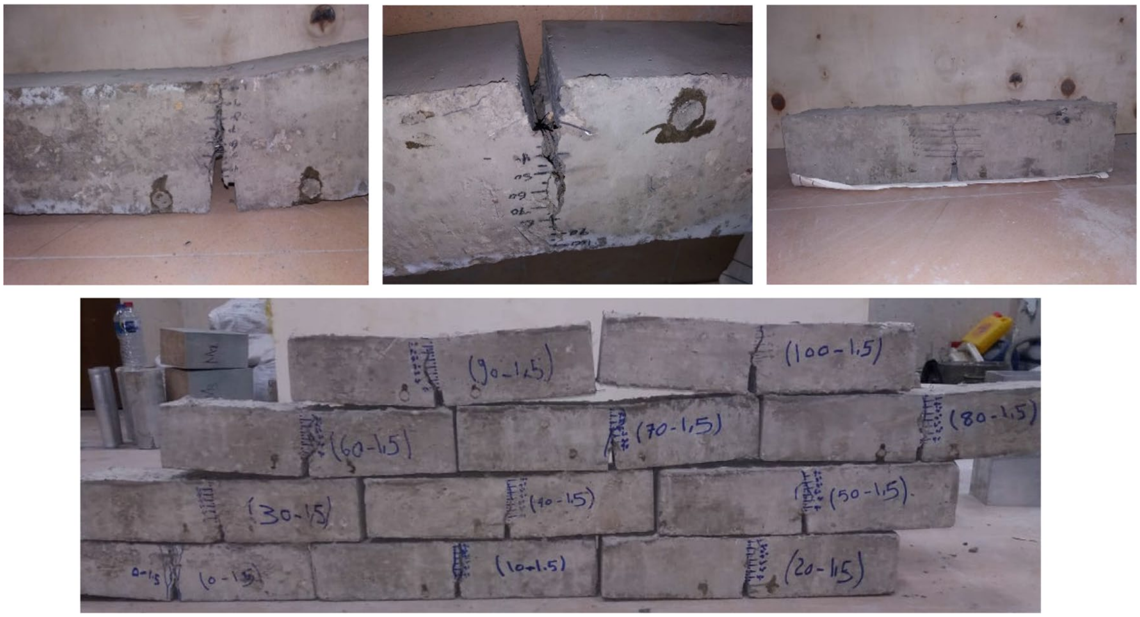

Fig. 9 Mode of failure of notched beam specimens

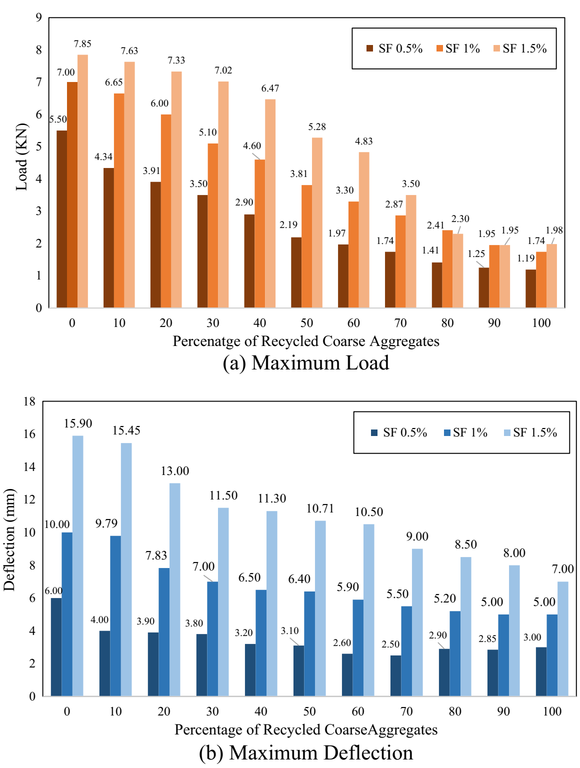

Fig. 10 Test results of tested specimens: (**a**) maximum loads and (**b**) maximum deflection

the number of steel fibers to 1.5%, the SFs in the sample enhanced the max load by 43% and 66.4% for NC and 100% RA replacement, respectively, compared with the 0.5% SF specimen. From Fig. 10b, it could be observed that raising the substitution level of recycled aggregate reduced the highest mid-span deflection by 50% for all specimens with various steel fiber ratios. Increasing the steel fiber quantity to 1.5% SF sample enhanced the max deflection by 165% and 133% for NC and 100% RA replacement, respectively, compared with the 0.5% SF specimen.

4.4 Crack Mouth Opening Displacement (CMOD)

The process of increasing and spreading cracks in concrete fibers is affected by the presence of the phenomenon of bridging in concrete, which depends on the bonding between the fibers and the concrete matrix as well as on the type of fibers and the axial tensile strength of the fibers. Crack mouth opening displacements at the peak load were recorded for different fiber contents, as presented in Table 3. Fig. 11 shows the load–crack mouth opening displacement relationships for beam specimens with various fiber types. A decrease in the peak load of samples was noted by raising the substitution level of recycled aggregates. At a similar level of loading (Fig. 12), samples with high fiber content endured less CMOD with low instability. The notch height had a considerable proportional impact on CMOD, where samples with 1.5% steel fibers experienced fewer values than those with 0.5% and 1% at a similar load level. The final values diverged according to the load-carrying capability of every beam sample. As the substitution level of recycled aggregates increased, the peak load decreased. A reduction in peak load could be associated with the lower strength of recycled aggregates because of the attached mortar (Ghorbel & Wardeh, 2017; Khafaga, 2014; Matar & Assaad, 2019). Steel fibers reinforced concrete samples displayed ductile response and recovered the load even after minimal post-crack loading. The post-peak response of steel fiber-reinforced recycled aggregate concrete was steep compared to steel fiber-reinforced standard concrete. This could be ascribed to the low number of cracks in the binder's matrix and the high quantity of breaking in recycled concrete aggregates. The steel fibers could sustain the load even at high peaks with a specific percentage of recycled aggregates. The CMOD curves of reference, steel fiber-reinforced standard, and recycled aggregate concrete samples also depicted the scattering of outcomes. As noted by past researchers, this scattering is associated with the dispersion, orientation, and quantity of steel fibers on the beam notch.

5 Linear Elastic Fracture Mechanics Analysis

Based on displacement control loading of samples, J-integral (J_{IC}), characteristic length (l_{ch}), fracture toughness (K_{IC}), brittleness (B), and fracture energy (G_F) were estimated.

$$K_{IC} = \frac{3\text{Pl}}{2bd^2} * \sqrt{a} * \left(1.93 - 3.07A + 14.53A^2 - 25.11A^3 + 25.8A^4\right) \tag{1}$$

The development of the main model for a material that the fracture parameters require was utilized to be measured analytically for concrete (Eq. 1) (Casuccio et al., 2008; Kazmi et al., 2018).Here, $A = (a/d)$, is the span length of the beam l (mm), P is the highest load (N), d is the height of the beam (mm), b is the width of the beam (mm), and a is the height of the notch (mm).

$$G_F = \frac{w_o + mg\delta_0}{A_{\text{lig}}} \tag{2}$$

$$G_F = \int_{\delta=0}^{\delta=\delta_{\text{lim}}} \sigma\, d\delta \tag{3}$$

$$G_F = \frac{K_{\text{IC}}^2}{E} \tag{4}$$

$$G_F = 2.5\,\alpha_0 \left(\frac{f_c}{0.051}\right)^{0.46} \left(1 + \frac{D_{\max}}{11.27}\right)^{0.22} \left(\frac{w}{c}\right)^{-0.30} \tag{5}$$

$$G_F = \left(0.0469\, D^2{}_{\max} - 0.5\, D_{\max} + 26\right) \left(\frac{f_c}{10}\right)^{0.7} \tag{6}$$

The G_F was assessed by five different models (Eqs. 2, 3, 4, 5, and 6) by Irwin (Bažant, 1997) and Bazant (Casuccio et al., 2008).Here, $\sigma = \frac{3Pl}{2b(h-a_0)^2}$, a_0 is the height of the notch (mm), d is the height of the beam (mm), b is the width of the beam (mm), P is the maximum load (N), and ɩ is the span length of the beam (mm).

CEB-FIP (Brown & Srawley, 1996) proposed (Eq. 5) to estimate the fracture energy of concrete in terms of the compressive strength and the maximum aggregate size.

Bazant and Becq-Giraduon (Irwin, 1957) proposed (Eq. 6) for the fracture energy of concrete as CEB-FIP and the addition of the water-to-cement ratio of the concrete. The equation has a water-to-cement ratio that is relevant to concrete.

Here, $D_{\max}$ is the highest size of aggregate (mm), f_c is the concrete's compression strength (MPa), a_0 is the aggregate's shape factor ($a_0 = 1$ for rounded aggregates, $a_0 = 1.44$ for angular aggregates), and w/c is the concrete's water–cement ratio.

$$l_{\text{ch}} = \frac{G_F E}{f_t^{\,2}} \tag{7}$$

$$B = \frac{L f_t^{\,2}}{G_F E} \tag{8}$$

$$J_{\text{IC}} = \frac{K_{IC}}{E} \tag{9}$$

The l_{ch}, B, and J_{IC} were assessed by utilizing the equations (Eqs. 7, 8, and 9) by Bazant (Casuccio et al., 2008) and Rice (CEB-FIP, 1990).

Here, L is the span of the test sample, E is the modulus of elasticity, ft is the tensile strength, and G_F is the fracture energy.

5.1 Fracture Response

Table 4, Figs. 13 and 14 show the computed fracture parameters per the terminologies stated in (Eqs. 1–9) for

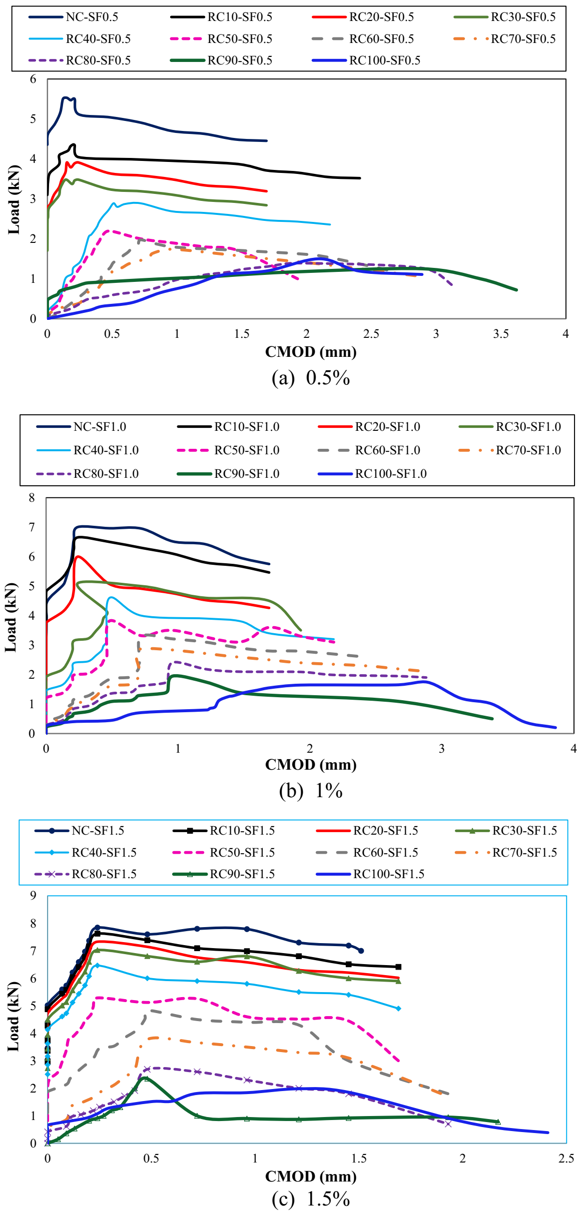

Fig. 11 Load- CMOD relationships of beam samples reinforced with different steel fibers ratios: (**a**) 0.5%, (**b**) 1.0%,and (**c**) 1.5%

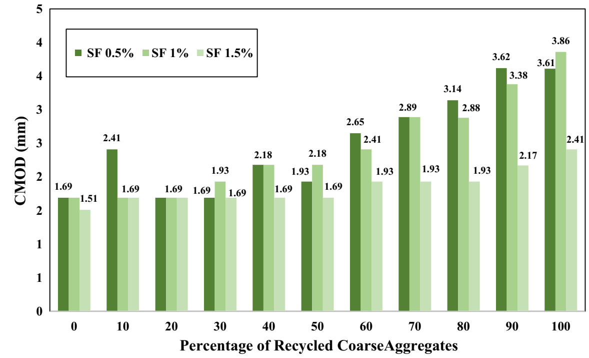

Fig. 12 CMOD at failure load–specimen ID

the notched beam samples with 0.5%, 1%, and 1.5% steel fibers.

5.2 Fracture Toughness (*KIC*) and Fracture Energy (*GF*)

Fig. 13 presents the outcomes of K_{IC} and G_F (as per Eq. (2)) for different recycled aggregate specimens. The K_{IC} is concrete type, recycled aggregate replacement ratio, and steel fibers content dependent, as shown in Fig. 13. The effect of using different recycled aggregate replacements (0%, 10%, to 100%) on K_{IC} was considered through beam samples with concrete mix ID (NC, RC10 to RC100), correspondingly. From Fig. 13a, it could be observed that raising the substitution level of recycled aggregate to 100% reduced the average K_{IC} by 77% for all steel fiber ratios. This could be ascribed to the reduction in compression strength and the enhancement in splitting tensile strength.

Regarding 0% mm and 100% aggregate replacement with various steel fibers ratios (0.5%, 1%, and 1.5%), it could be observed that raising the steel fiber ratio enhanced the KIC by 43% and 66.4%, respectively. The steel fibers had a high elastic modulus and better flexibility, which can improve fracture toughness; the fibrillated steel fibers can be distributed uniformly in specimens. The fiber could reduce the concentration of stresses on the top of the cracks and enhance the resistance against crack development (Bazant & Becq-Giraudon, 2002; Cuenca & Ferrara, 2020; Rice, 1968). The number of steel fibers governed the cracking behavior. The G_F for recycled aggregate concrete is reliant on steel fibers content, as presented in the experimental outcomes shown in Fig. 13b. Fig. 13b depicts the evaluation of G_F for various samples. It could be observed that using 100% substitution of RA for the sample without replacement reduced the average G_F by 95% for replacement aggregate compared with the natural aggregate specimen. Raising the steel fibers quantity to 1.5%, SFs in the sample enhanced the GF by 286% and 100% for NC and 100% RA replacement, correspondingly in comparison with 0.5% SFs in the concrete sample. These characteristics could be observed in specimens with 0.5% steel fibers, and an inverse tendency could be observed with other samples. The larger the dose of fibers, the stronger the restraint of the steel fibers is, and GF gets higher and higher.

The fracture energy of recycled aggregate concrete (for a 100% substitution level of recycled aggregates) revealed a 40% decrease with respect to standard concrete. The reduction in fracture energy of recycled aggregate concrete could be connected with the low strength

Table 4 Fracture parameters of the notched beam samples with various steel fiber content

Parameter		K_{IC}	G_F					l_{ch}	B	J_{IC}
		$N/mm^{3/2}$	N/mm					m		N/mm
Notch	Concrete ID	Equation (1)	Equation (2)	Equation (3)	Equation (4)	Equation (5)	Equation (6)	Equation (7)	Equation (8)	Equation (9)
G1	NC-SF0.5	80.66	27.61	44.11	13.34	8.56	59.22	8.86	0.05	0.17
	RC10-SF0.5	63.65	14.28	23.20	7.02	8.36	58.30	5.73	0.05	0.11
	RC20-SF0.5	57.34	12.12	20.38	6.16	8.15	57.35	4.79	0.05	0.11
	RC30-SF0.5	51.33	10.45	17.78	5.38	7.94	56.39	3.99	0.05	0.10
	RC40-SF0.5	42.53	6.85	12.40	3.75	7.79	55.69	2.83	0.05	0.09
	RC50-SF0.5	32.12	4.44	9.07	2.74	7.61	54.84	1.68	0.06	0.09
	RC60-SF0.5	28.89	3.53	6.85	2.07	7.37	53.68	1.41	0.06	0.07
	RC70-SF0.5	25.52	2.74	5.81	1.76	7.34	53.53	1.13	0.06	0.07
	RC80-SF0.5	20.68	2.84	5.47	1.65	7.09	52.34	0.76	0.06	0.08
	RC90-SF0.5	18.33	2.37	4.76	1.44	6.84	51.11	0.64	0.06	0.08
	RC100-SF0.5	17.45	2.14	4.77	1.44	6.58	49.85	0.62	0.07	0.08
G2	NC-SF1.0	102.66	56.97	93.56	28.30	8.73	60.00	13.94	0.05	0.28
	RC10-SF1.0	97.52	52.77	87.02	26.32	8.56	59.22	12.95	0.05	0.27
	RC20-SF1.0	87.99	32.53	62.79	18.99	8.30	58.03	11.03	0.06	0.22
	RC30-SF1.0	74.79	28.43	47.72	14.43	8.06	56.94	8.28	0.05	0.19
	RC40-SF1.0	67.46	22.09	39.96	12.09	7.97	56.53	6.84	0.05	0.18
	RC50-SF1.0	55.87	19.53	32.59	9.86	7.70	55.27	4.96	0.05	0.18
	RC60-SF1.0	48.40	14.97	26.02	7.87	7.52	54.41	3.84	0.05	0.16
	RC70-SF1.0	42.09	11.93	21.10	6.38	7.28	53.24	3.10	0.05	0.15
	RC80-SF1.0	35.34	7.60	16.75	5.07	7.09	52.34	2.24	0.07	0.14
	RC90-SF1.0	28.60	6.00	13.03	3.94	6.84	51.11	1.56	0.07	0.14
	RC100-SF1.0	25.52	4.39	11.63	3.52	6.65	50.16	1.35	0.08	0.14

Table 4 (continued)

Parameter		K_{IC}	G_F					l_{ch}	B	J_{IC}
		N/mm$^{3/2}$	N/mm					m		N/mm
Notch	Concrete ID	Equation (1)	Equation (2)	Equation (3)	Equation (4)	Equation (5)	Equation (6)	Equation (7)	Equation (8)	Equation (9)
G3	NC-SF1.5	115.12	106.60	166.83	50.46	9.32	62.64	15.98	0.05	0.44
	RC10-SF1.5	111.90	98.80	157.56	47.66	9.15	61.90	15.41	0.05	0.43
	RC20-SF1.5	107.50	80.72	127.36	38.52	9.01	61.27	14.74	0.05	0.36
	RC30-SF1.5	102.95	66.77	107.90	32.64	8.84	60.51	13.81	0.05	0.32
	RC40-SF1.5	94.88	58.98	97.72	29.56	8.64	59.61	12.26	0.05	0.31
	RC50-SF1.5	77.43	39.41	75.58	22.86	8.41	58.56	8.35	0.06	0.30
	RC60-SF1.5	70.83	34.40	67.79	20.50	8.00	56.67	7.54	0.06	0.29
	RC70-SF1.5	51.33	15.68	42.10	12.73	7.64	54.98	4.28	0.08	0.25
	RC80-SF1.5	33.73	8.30	26.13	7.90	7.46	54.12	1.90	0.10	0.23
	RC90-SF1.5	28.60	2.03	20.85	6.31	7.37	53.68	1.42	0.31	0.22
	RC100-SF1.5	29.04	1.98	18.53	5.60	7.09	52.34	1.53	0.28	0.19

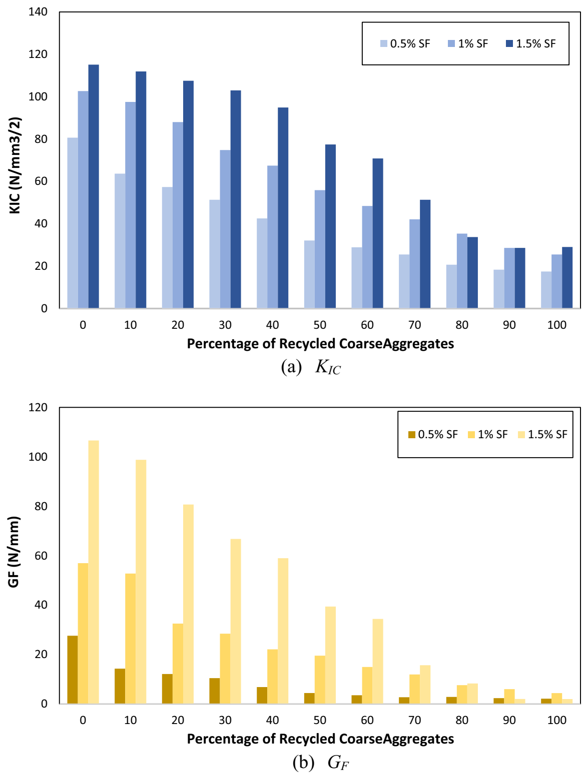

Fig. 13 Fracture characteristics of all the testesd specimens: (**a**) K_{IC} and (**b**) G_F

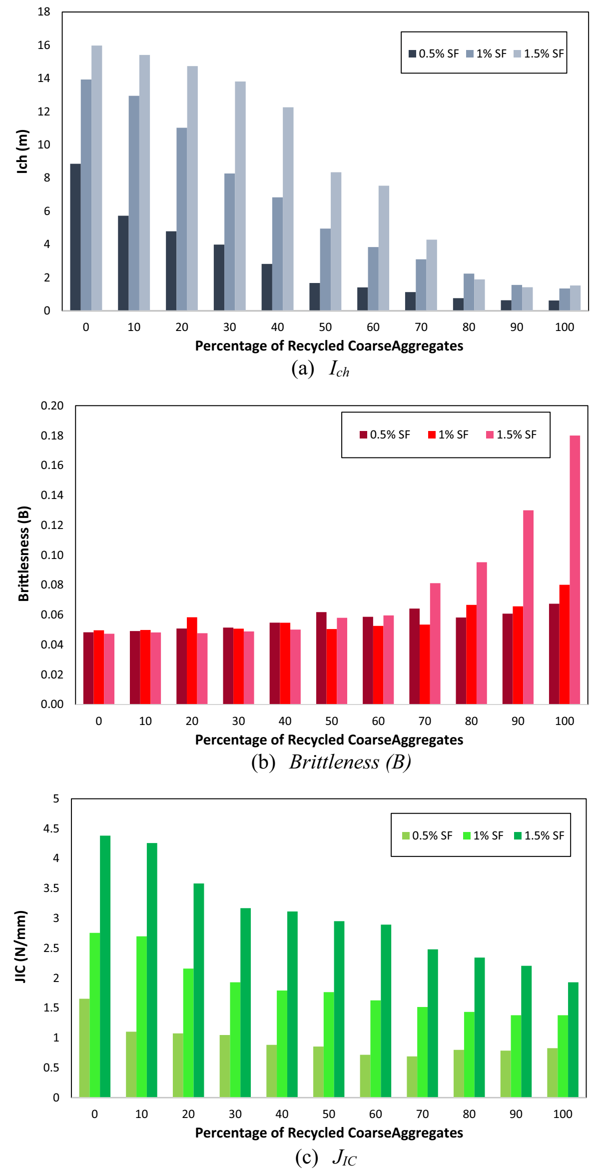

Fig. 14 (**a**) Characteristic length (l_{ch}), (**b**) brittleness (*B*), and (**c**) J- integral J_{IC} of beam specimens

of recycled aggregates, which reduced the splitting and twisting of cracks during failure. Because of the steel fibers in concrete samples, cracking cannot propagate without stretching and de-bonding the steel fibers, leading to an improved G_f of the concrete sample (Alberti et al., 2014; Arslan 2016; Biolzi & Cattaneo 2017; Pająk & Ponikiewski 2017; Buratti et al., 2011; Wang et al., 1994). A rise in fracture energy signifies). A rise in fracture energy signifies the enhancement in energy dissipation and ductility of standard and recycled aggregate concrete with manufactured fibers. The inclusion of steel fibers enhances energy absorption, such as concrete's toughness, by bridging the behavior of fiber. The toughness of concrete with steel fibers was noted to be higher than that of standard concrete. Hence, the fracture and toughness of standard and recycled aggregate concrete could be enhanced by including steel fibers.

5.3 Characteristic Length (l_{ch}), Brittleness (*B*), and J-Integral (*JIC*)

Fig. 14 shows the results of l_{ch}, *B*, and J_{IC} for various notch height beam specimens. The parameters l_{ch}, *B*, and $J_{IC,}$ are given by Eqs. (7), (8), and (9), respectively. Fig. 14a presents the outcomes of the l_{ch} for different percentages of recycled aggregate in different samples of beams. It could be observed that specimens using various aggregate ratios, raising the substitution level to 100%, reduced the l_{ch} by 92% for different steel fiber ratios. Nevertheless, increasing the steel fiber content enhanced the l_{ch} by 80.4% and 147% for 0% and 100% aggregate replacement ratios, respectively. Fig. 14c presents the outcomes of the J_{IC} for different percentages of recycled aggregate in different samples of beams. It could be observed that using 100% RA substitution for the sample reduced the J_{IC} by 52% for all replacement ratios compared to the specimen without aggregate replacement. Nonetheless, raising the number of steel fibers for specimens increased the J_{IC} by 165% and 136% for 0% and 100% aggregate replacement ratios, respectively, compared with a 0.5% steel fiber ratio. Among them, l_{ch}, B, and J_{IC} of concrete with 1.5% steel fibers were significantly improved.

6 Conclusions

Based on the experimental results and discussion of the recycled aggregate concrete notched beam samples, the following points are decided:

1. Using 100% recycled aggregate as a substitute for aggregate weight in concrete effectively reduced the strength characteristics after 28 days. The reductions were 33%, 19%, and 75% for compression strength, flexural strength, and splitting tensile strength, correspondingly.
2. The presence of 1.5% steel fibers enhanced the maximum failure load for beam samples with and without 100% recycled aggregate replacement by 43% and 66.4%, respectively, compared with 0.5% steel fiber specimens. Also, the maximum mid-span deflection increased by 165% and 133%, respectively.
3. There is a significant difference among the projections of the fracture energy after the theoretical LEFM formula for fracture toughness, fracture energy, and characteristic length. It could be noted that the "by definition" work procedure was the most reliable, as the nonlinearity is associated with the manners.
4. The addition of recycled aggregate as a replacement for natural aggregate reduced the fracture parameters, i.e., fracture toughness (K_{IC}), fracture energy (G_F), characteristic length (l_{ch}), and J-integral (J_{IC}) by 77%, 95%, 92%, and 52%, respectively. On the contrary, the fracture parameters were significantly enhanced due to the presence of 1% steel fiber by 43%, 286%, 80%, and 165% higher than conventional concrete, while their counterparts at a 1.5% steel fiber ratio were 65%, 100%, 147%, and 136%, respectively.

Acknowledgements

The authors are thankful to the Deanship of Scientific Research at Najran University for funding this work under the Research Groups Funding program grant code (NU/RG/SERC/12/17).

Author contributions

AMM: conceptualization, methodology, idea of the research, writing, writing—review and editing. WM: conceptualization, methodology, idea of the research, writing, writing—review, supervision and editing. BT: conceptualization, methodology, idea of the research, writing, writing—review and editing. ME: conceptualization, methodology, idea of the research, writing, writing—review and editing. AMY: writing and writing—review. SF: conceptualization, methodology, idea of the research, writing, writing—review, supervision and editing.

Availability of data and materials

Some of all the data, models, or code that support the findings of this study are available from the corresponding author upon reasonable request.

Declarations

Ethics approval and consent to participate

None.

Consent for publication

None.

Competing interests

No potential competing interest was reported by the authors.

Received: 28 February 2023 Accepted: 26 August 2023
Published online: 13 November 2023

References

ACI Committee 446, "Fracture Mechanics of Concrete: Concepts, Models, and Determination of Material Properties (ACI 446.1R-91)," American Concrete Institute, Farmington Hills, MI, 1991, pp. 146.

Aflaki Samani, M., & Jabbari Lak, S. (2019). Experimental investigation on the mechanical properties of recycled aggregate concrete reinforced by waste carbon fibers. *International Journal of Environmental Science and Technology, 16*(8), 4519–4530.

Afroughsabet, V., Biolzi, L., & Ozbakkaloglu, T. (2017). Influence of double hooked-end steel fibers and slag on mechanical and durability properties of high performance recycled aggregate concrete. *Composite Structures., 181*, 273–284. https://doi.org/10.1016/j.compstruct.2017.08.086

Ahmadi, M., & Farzin, S. (2017). Mechanical properties of the concrete containing recycled fibers and aggregates. *Construction and Building Materials, 144*, 392–398. https://doi.org/10.1016/j.conbuildmat.2017.03.215

Alberti, M. G., Enfedaque, A., Gálvez, J. C., Cánovas, M. F., & Osorio, I. R. (2014). Polyolefin fiber-reinforced concrete enhanced with steel-hooked fibers in low proportions. *Materials & Design, 60*, 57–65.

Ali, B., Raza, S. S., Kurda, R., & Alyousef, R. (2021). Synergistic effects of fly ash and hooked steel fibers on strength and durability properties of high strength recycled aggregate concrete. *Resources, Conservation and Recycling, 168*, 105444.

Althoey, F., Zaid, O., de Prado-Gil, J., Palencia, C., Ali, E., Hakeem, I., & Martínez-García, R. (2022). Impact of sulfate activation of rice husk ash on the performance of high strength steel fiber reinforced recycled aggregate concrete. *Journal of Building Engineering, 54*, 104610.

Arslan, M. E. (2016). Effects of basalt and glass chopped fibers addition on fracture energy and mechanical properties of ordinary concrete: CMOD measurement. *Construction and Building Materials, 114*, 383–391. https://doi.org/10.1016/j.conbuildmat.2016.03.176

ASTM Annual Book of Standards, Vol. 04.01 Cement; Lime; Gypsum, American Society for Testing and Materials, West Conshohocken, PA, 2004.

ASTM C 496/-11. (2011). Standard Test Method for Splitting Tensile Strength of Cylindrical Concrete Specimens.

ASTM:C494/C494M-13 Standard Specification for Chemical Admixtures for Concrete. ASTM International, West Conshohocken, USA, 2013.

ASTM-C33 Standard specification for concrete aggregates. ASTM International, West Conshohocken

Baena, M., Torres, L., Turon, A., Llorens, M., & Barris, C. (2016). Bond behaviour between recycled aggregate concrete and glass fibre reinforced polymer bars. *Construction and Building Materials, 106*, 449–460.

Baraghith, A. T., Mansour, W., Behiry, R. N., & Fayed, S. (2022). Effectiveness of SHCC strips reinforced with glass fiber textile mesh layers for shear strengthening of RC beams: Experimental and numerical assessments. *Construction and Building Materials, 327*, 127036.

Basha, A., Fayed, S., & Mansour, W. (2020). Flexural strengthening of RC one way solid slab with strain hardening cementitious composites (SHCC). *Advances in Concrete Construction, 9*(5), 511–527.

Bažant, Z. P. (1997). Scaling of quasibrittle fracture: asymptotic analysis. *International Journal of Fracture, 83*, 19–40. https://doi.org/10.1023/A:1007387823522

Bazant, Z. P., & Becq-Giraudon, E. (2002). Statistical prediction of fracture parameters of concrete and implications for choice of testing standard. *Cement and Concrete Research, 32*(4), 529–556. https://doi.org/10.1016/s0008-8846(01)00723-2

Biolzi, L., & Cattaneo, S. (2017). Response of steel fiber reinforced high strength concrete beams: Experiments and code predictions. *Cement and Concrete Composites, 77*, 1–13. https://doi.org/10.1016/j.cemconcomp.2016.12.002

Brown, W.F., Srawley, J.E. (1966). Plane strain crack toughness testing of high strength metallic materials.

Buratti, N., Mazzotti, C., & Savoia, M. (2011). Post-cracking behaviour of steel and macro-synthetic fibre-reinforced concretes. *Construction and Building Materials, 25*, 2713–2722. https://doi.org/10.1016/j.conbuildmat.2010.12.022

Carneiro, J. A., Lima, P. R. L., Leite, M. B., & Toledo Filho, R. D. (2014). Compressive stress–strain behavior of steel fiber reinforced-recycled aggregate concrete. *Cement and Concrete Composites, 46*, 65–72.

Casuccio, M., Torrijos, M. C., Giaccio, G., & Zerbino, R. (2008). Failure mechanism of recycled aggregate concrete. *Construction and Building Materials, 22*, 1500–1506. https://doi.org/10.1016/j.conbuildmat.2007.03.032

CEB-FIP. (1990). Model code for concrete structures. *Bulletin D'information, 199*, 1991.

Chaboki, H. R., Ghalehnovi, M., Karimipour, A., & De Brito, J. (2018). Experimental study on the flexural behaviour and ductility ratio of steel fibres coarse recycled aggregate concrete beams. *Construction and Building Materials, 2018*(186), 400–422.

Corinaldesi, V., & Moriconi, G. (2009). Behaviour of cementitious mortars containing different kinds of recycled aggregate. *Construction and Building Materials, 23*(1), 289–294.

Cuenca, E., & Ferrara, L. (2020). Fracture toughness parameters to assess crack healing capacity of fiber reinforced concrete under repeated cracking-healing cycles. *Theoretical and Applied Fracture Mechanics, 106*, 102468. https://doi.org/10.1016/j.tafmec.2019.102468

"Egyptian Code of Practice for Design and Construction of concrete structure code", Standing Committee to prepare the Egyptian, HBRC, Cairo 2019. (2019) ECP 203/2019

EN BS 12390-3. (2002). Testing hardened concrete; part 3: compressive strength of test specimens. Br Stand Inst.

Fayed, S., Badr el-din, A., Basha, A., & Mansour, W. (2022e). Shear behavior of RC pile cap beams strengthened using ultra-high performance concrete reinforced with steel mesh fabric. *Case Studies in Construction Materials, 17*, e01532.

Fayed, S., & Mansour, W. (2020). Evaluate the effect of steel, polypropylene and recycled plastic fibers on concrete properties. *Advances in Concrete Construction, 10*(4), 319–332.

Ghorbel, E., & Wardeh, G. (2017). Influence of recycled coarse aggregates incorporation on the fracture properties of concrete. *Construction and Building Materials, 154*, 51–60. https://doi.org/10.1016/j.conbuildmat.2017.07.183

Hamoda, A., Emara, M., & Mansour, W. (2019). Behavior of steel I-beam embedded in normal and steel fiber reinforced concrete incorporating demountable bolted connectors. *J Composites Part B: Engineering, 174*, 106996.

Irwin, G. R. (1957). Analysis of stresses and strains near the end of a crack traversing a plate.

Kapoor, K., Singh, S. P., & Singh, B. (2016). Durability of self-compacting concrete made with Recycled Concrete Aggregates and mineral admixtures. *Construction and Building Materials, 128*, 67–76. https://doi.org/10.1016/j.conbuildmat.2016.10.026

Kazmi, S. M. S., Munir, M. J., Wu, Y.-F., & Patnaikuni, I. (2018). Effect of macro-synthetic fibers on the fracture energy and mechanical behavior of recycled aggregate concrete. *Construction and Building Materials, 189*, 857–868. https://doi.org/10.1016/j.conbuildmat.2018.08.161

Khafaga, S. A. (2014). Production of high strength self compacting concrete using recycled concrete as fine and/or coarse aggregates. *World Applied Sciences Journal, 29*, 465–474. https://doi.org/10.5829/idosi.wasj.2014.29.04.13861

Kurad, R., Silvestre, J. D., de Brito, J., & Ahmed, H. (2017). Effect of incorporation of high volume of recycled concrete aggregates and fly ash on the strength and global warming potential of concrete. *Journal of Cleaner Production, 166*, 485–502.

Liu, X., Yan, M., Galobardes, I., & Sikora, K. (2018). Assessing the potential of functionally graded concrete using fibre reinforced and recycled aggregate concrete. *Construction and Building Materials, 171*, 793–801. https://doi.org/10.1016/j.conbuildmat.2018.03.202

Mansour, W. (2021). Numerical analysis of the shear behavior of FRP-strengthened continuous RC beams having web openings. *Engineering Structures, 227*, 111451.

Mansour, W., & Fayed, S. (2021a). Effect of interfacial surface preparation technique on bond characteristics of both NSC-UHPFRC and NSC-NSC composites. *Structures, 29*, 147–166.

Mansour, W., & Fayed, S. (2021b). Flexural rigidity and ductility of RC beams reinforced with steel and recycled plastic fibers. *Steel and Composite Structures, 41*(3), 317–334.

Mansour, W., Sakr, M. A., Seleemah, A. A., Tayeh, B. A., & Khalifa, T. M. (2022a). Bond behavior between concrete and prefabricated ultra high-performance fiber-reinforced Concrete (UHPFRC) plates. *Structural Engineering and Mechanics, 81*(3), 305–316.

Mansour, W., Tayeh, B. A., & Tam, L.-H. (2022b). Finite element analysis of shear performance of UHPFRC-encased steel composite beams: Parametric study. *Engineering Structures, 271*, 114940.

Masood, B., Elahi, A., Barbhuiya, S., & Ali, B. (2020). Mechanical and durability performance of recycled aggregate concrete incorporating low calcium bentonite. *Construction and Building Materials, 237*, 117760.

Matar, P., & Assaad, J. J. (2019). Concurrent effects of recycled aggregates and polypropylene fibers on workability and key strength properties of self-consolidating concrete. *Construction and Building Materials, 199*, 492–500.

Pająk, M., & Ponikiewski, T. (2017). Investigation on concrete reinforced with two types of hooked fibers under flexure. *Procedia Engineering, 193*, 128–135. https://doi.org/10.1016/j.proeng.2017.06.195

Pedro, D., De Brito, J., & Evangelista, L. (2017). Evaluation of high-performance concrete with recycled aggregates: Use of densified silica fume as cement replacement. *Construction and Building Materials, 147*, 803–814.

Pepe, M., Toledo Filho, R. D., Koenders, E. A. B., & Martinelli, E. (2014). Alternative processing procedures for recycled aggregates in structural concrete. *Construction and Building Materials, 69*, 124–132. https://doi.org/10.1016/j.conbuildmat.2014.06.084

Rajhans, P., Chand, G., Kisku, N., Panda, S. K., & Nayak, S. (2019). Proposed mix design method for producing sustainable self compacting heat cured recycled aggregate concrete and its microstructural investigation. *Construction and Building Materials, 218*, 568–581.

Rice, J. (1968). A path integral and the approximate analysis of strain concentration by notches and cracks. *Journal of Applied Mechanics, 35*, 379–386. https://doi.org/10.1115/1.3601206

Sagoe-Crentsil, K. K., Brown, T., & Taylor, A. H. (2001). Performance of concrete made with commercially produced coarse recycled concrete aggregate. *Cement Concrete Research, 31*, 707–712. https://doi.org/10.1016/S0008-8846(00)00476-2

Sakr, M. A., Sleemah, A.A., Khalifa, T.M., Mansour, W.N. (2018). Behavior of RC beams strengthened in shear with ultra-high performance fiber reinforced concrete (UHPFRC), *MATEC web of conferences, EDP Sciences*, p. 09002.

Singh, N., & Singh, S. P. (2016). Carbonation and electrical resistance of self compacting concrete made with recycled concrete aggregates and metakaolin. *Construction and Building Materials, 121*, 400–409.

Wang, Y., Zureick, A.-H., Cho, B.-S., & Scott, D. E. (1994). Properties of fibre reinforced concrete using recycled fibres from carpet industrial waste. *Journal of Materials Science, 29*, 4191–4199. https://doi.org/10.1007/BF00414198

Xie, J. H., Guo, Y. C., Liu, L. S., & Xie, Z. H. (2015). Compressive and flexural behaviours of a new steel-fibre-reinforced recycled aggregate concrete with crumb rubber. *Construction and Building Materials, 79*, 263–272.

Zaid, O., Martínez-García, R., Abadel, A. A., Fraile-Fernández, F. J., Alshaikh, I. M., & Palencia-Coto, C. (2022a). To determine the performance of metakaolin-based fiber-reinforced geopolymer concrete with recycled aggregates. *Archives of Civil and Mechanical Engineering, 22*(3), 1–14.

Zaid, O., Mukhtar, F. M., Rebeca, M., El Sherbiny, M. G., & Mohamed, A. M. (2022b). Characteristics of high-performance steel fiber reinforced recycled aggregate concrete utilizing mineral filler. *Case Studies in Construction Materials, 16*, e00939.

Publisher's Note

Ahmed M. Maglad Assistant Professor, PhD, Department of Civil Engineering, Najran University, Najran, Saudi Arabia.

Walid Mansour Assistant Professor, PhD, Civil Engineering Department, Faculty of Engineering, Kafrelsheikh University, Kafrelsheikh 33511, Egypt.

Bassam A. Tayeh Professor, PhD, Civil Engineering Department, Faculty of Engineering, Islamic University of Gaza, Gaza, Palestine.

Mohamed Elmasry Assistant Professor, PhD, High Institute of Engineering, Elshorouk Academy, Cairo, Egypt.

Ahmed. M. Yosri Assistant Professor, PhD, Civil Engineering Department, Faculty of Engineering, Delta University for Science and Technology, Belkas, Egypt.

Sabry Fayed Associate Professor, PhD, Civil Engineering Department, Faculty of Engineering, Kafrelsheikh University, Kafrelsheikh 33511, Egypt.